

Manuscript Number: JEMBE-D-15-00533R1

Title: Application of computer-aided tomography techniques to visualise kelp holdfast structure reveals the importance of habitat complexity for supporting marine biodiversity.

Article Type: Full Length Article

Keywords: Ecosystem engineer
Fractal
Image analysis
Kelp holdfasts
Benthic fauna
Laminaria hyperborea

Corresponding Author: Ms. Chloé Orland,

Corresponding Author's Institution: University of Cambridge

First Author: Chloé Orland

Order of Authors: Chloé Orland; Ana M Queirós; John I Spicer; Caroline L McNeill; Sarah Higgins; Sharon Goldworthy; Tony Zananiri; Lesley Archer ; Stephen Widdicombe, PhD

Abstract: Ecosystem engineers that increase habitat complexity are keystone species in marine systems, increasing shelter and niche availability, and therefore biodiversity. For example, kelp holdfasts form intricate structures and host the largest number of organisms in kelp ecosystems. However, methods that quantify 3D habitat complexity have only seldom been used in marine habitats, and never in kelp holdfast communities. This study investigated the role of kelp holdfasts (*Laminaria hyperborea*) in supporting benthic faunal biodiversity. Computer-aided tomography scanning (CT-) was used to quantify the three-dimensional geometrical complexity of holdfasts, including volume, surface area and surface fractal dimension (FD). Additionally, the number of haptera, number of haptera per unit of volume, and age of kelps were estimated. These measurements were compared to faunal biodiversity and community structure, using partial least-squares regression and multivariate ordination. Holdfast volume explained most of the variance observed in biodiversity indices, however all other complexity measures also strongly contributed to the variance observed. Multivariate ordinations further revealed that surface area and haptera per unit of volume accounted for the patterns observed in faunal community structure. Using 3D image analysis, this study makes a strong contribution to elucidate quantitative mechanisms underlying the observed relationship between biodiversity and habitat complexity. Furthermore, the potential of CT-scanning as an ecological tool is demonstrated, and a methodology for its use in future similar studies is established. Such spatially resolved imager analysis could help identify structurally complex areas as biodiversity hotspots, and may support the prioritization of areas for conservation.

11th December 2015

Dear Dr Shumway,

We have submitted the manuscript "*Application of computer-aided tomography techniques to visualise kelp holdfast structure reveals the importance of habitat complexity for supporting marine biodiversity*", which we believe to be of high relevance to your readership. We introduce a novel approach to quantifying three-dimensional complexity in kelp habitats, an attribute of marine systems widely recognized as having a fundamental role in the sustenance of marine biodiversity, but seldom quantitatively assessed. This work helps to elucidate, in a quantitative manner, the mechanisms underlying biodiversity and kelp 3D complexity. As such, this study is of great relevance to ecologists concerned with the conservation of biodiversity, particularly given the recent interest in the role of kelp beds as hot-spots for marine life.

We introduce computer aided tomography (CT-scanning) as an ecological tool with great potential for development in the context of quantifying 3D complexity in kelp habitats, having recently been used with success in sedimentary habitats (Mazik et al. 2008). Further, we provide the mathematical protocol to quantify 3D complexity of holdfasts, by using fractal dimensions and borrowing 3D autocorrelation indices more commonly used in medicine. CT-scanning provides highly valuable information, and emerges as a unique tool to analyse habitat complexity quantitatively.

We present a study rich in innovative techniques, both in data acquisition and processing, and successfully demonstrate its wider potential for application in marine community and ecosystem research. We therefore believe that this study is a fitting contribution to JEMBE.

For the authors, with our kindest regards,

Chloé Orland

Department of Plant Sciences, University of Cambridge

Downing St, Cambridge

CB2 3EA, UK

+44 (0) 7837964164

co353@cam.ac.uk, orland.chloe@gmail.com

Cambridge, January 3rd 2016

Dear Mrs. Shumway,

I have modified the 5 figures according to your recommendations. I hope the manuscript is now fit for publication.

Sincerely yours,
Chloé Orland

Highlights

- CT-scanning was used for fine scale quantification of the 3D geometrical complexity of kelp holdfasts.
- Biodiversity was strongly affected by all measures of holdfast complexity.
- CT-scanning is an emerging and potentially powerful tool for ecological research.

1 **Application of computer-aided tomography techniques to visualize kelp holdfast**
2 **structure reveals the importance of habitat complexity for supporting marine**
3 **biodiversity**

4
5
6
7
8
9 5 **Chloé Orland^{1,2}, Ana M. Queirós¹, John I. Spicer², Caroline L. McNeill¹, Sarah**
10
11 6 **Higgins³, Sharon Goldworthy³, Tony Zananiri³, Lesley Archer³ and Stephen**
12
13 7 **Widdicombe¹**

14
15
16
17
18
19
20 10 **¹Plymouth Marine Laboratory, Prospect Place, West Hoe, Plymouth PL1 3DH, United Kingdom**

21
22 11 **²Marine Biology and Ecology Research Centre, School of Marine Science and Engineering,**
23
24 12 **Plymouth University, Drake Circus, Plymouth PL4 8AA, United Kingdom**

25
26
27 13 **³South Devon Healthcare NHS Foundation Trust, Torbay Hospital, Lawes Bridge, Torquay TQ2**
28
29 14 **7AA, United Kingdom**

30
31
32
33
34 16 **Corresponding author:**

35
36 17 **Chloé Orland, co353@cam.ac.uk, orland.chloe@gmail.com**

37
38 18 **Present address: Department of Plant Sciences, University of Cambridge, Downing**
39
40 19 **Street, Cambridge CB2 3EA, United Kingdom**

41
42
43
44
45
46
47
48
49
50
51
52
53

Author contributions: SW originally formulated the idea, CO and AMQ collaborated in developing
54 methodology, CO conducted fieldwork, SH, SG, TZ and LA generated scanned images, CO and CLM generated
55 biodiversity data, CO analyzed the images, developed the complexity indices and performed statistical analyses
56 in collaboration with AMQ, and CO, AMQ, SW and JIS wrote the manuscript.

57
58 **Abbreviations:** CT = computer-aided tomography, FD = fractal dimension
59
60
61
62
63
64
65

23 **Abstract** Ecosystem engineers that increase habitat complexity are keystone species in marine
24 systems, increasing shelter and niche availability, and therefore biodiversity. For example, kelp
25 holdfasts form intricate structures and host the largest number of organisms in kelp ecosystems.
26 However, methods that quantify 3D habitat complexity have only seldom been used in marine
27 habitats, and never in kelp holdfast communities. This study investigated the role of kelp holdfasts
28 (*Laminaria hyperborea*) in supporting benthic faunal biodiversity. Computer-aided tomography
29 scanning (CT-) was used to quantify the three-dimensional geometrical complexity of holdfasts,
30 including volume, surface area and surface fractal dimension (FD). Additionally, the number of
31 haptera, number of haptera per unit of volume, and age of kelps were estimated. These measurements
32 were compared to faunal biodiversity and community structure, using partial least-squares regression
33 and multivariate ordination. Holdfast volume explained most of the variance observed in biodiversity
34 indices, however all other complexity measures also strongly contributed to the variance observed.
35 Multivariate ordinations further revealed that surface area and haptera per unit of volume accounted
36 for the patterns observed in faunal community structure. Using 3D image analysis, this study makes a
37 strong contribution to elucidate quantitative mechanisms underlying the observed relationship between
38 biodiversity and habitat complexity. Furthermore, the potential of CT-scanning as an ecological tool is
39 demonstrated, and a methodology for its use in future similar studies is established. Such spatially
40 resolved imager analysis could help identify structurally complex areas as biodiversity hotspots, and
41 may support the prioritization of areas for conservation.

42
43
44 **Keywords** Ecosystem engineer · Fractal · Image analysis · Kelp holdfasts ·
45 Benthic fauna · *Laminaria hyperborea*
46
47

48 49 50 51 **1. Introduction**

52
53
54
55 The idea that habitat structure is a major influence on biodiversity (Simpson, 1949) is now well
56
57
58 accepted, and an increase in available surface area is considered to be the main explanation for the
59
60 positive correlations often observed between habitat structure and biodiversity (Connor and McCoy,
61
62
63
64
65

1 52 1979). This idea follows the classical theory of island biogeography (MacArthur and Wilson, 1967),
2 53 whereby they explained the effects of distance and area on biodiversity. Underpinning this relationship
3
4 54 is the understanding that the structural complexity of habitats regulates the distribution of refuges
5
6 55 available for protection, nesting, nurseries, mating and resting (Steneck et al., 2002), food resources
7
8 56 and foraging space, thus reducing competition and enabling the coexistence of a wide range of species
9
10 57 (Bell et al., 1991). Given that space is a limiting resource in many shallow marine systems, large
11
12 58 organisms which provide additional three-dimensional habitats, e.g. macrophytes (Blight and
13
14 59 Thompson, 2008), are typically seen as key or critical species in marine systems (Jones et al., 1994;
15
16 60 Wright and Jones, 2006; Hastings et al., 2007). As these large structure-forming organisms modify the
17
18 61 physical and chemical structure of habitats, they can be considered as ecosystem engineers (Jones et
19
20 62 al., 1994).

21
22
23
24 63 Kelps were one of the first groups of species identified as structurally enriching engineers, with the
25
26 64 loss of kelp forest due to grazing being recognized as a simplification of trophic complexity in near
27
28 65 shore systems (Estes et al., 1998). The physical presence of kelp has numerous positive effects on
29
30 66 species diversity by enhancing ecosystem stability spatially and temporally, modifying the distribution
31
32 67 and abundance of resources, as well as altering current speed, light availability and nutrient cycles
33
34 68 (Jones et al., 1997; Hastings et al., 2007). Therefore, identifying the physical attributes of macroalgae
35
36 69 that contribute to the maintenance of the kelp-associated community diversity will help to elucidate
37
38 70 the importance of keystone structures in marine habitats (Tews et al., 2004) and support conservation
39
40 71 measurements.

41
42
43
44 72 Within kelp habitats, it is the holdfast which provides the majority of intricate structures and hosts
45
46 73 a vast number of associated faunal species (Christie et al., 2003; Arroyo et al., 2004). The holdfast is
47
48 74 composed of numerous root-like haptera structures, entangling and creating spaces and gaps (Moore,
49
50 75 1972), with new, outer hapteron layers adding to the structure as the kelp ages (Smith et al., 1996).
51
52 76 Numerous studies have identified a relationship between holdfast size or volume and benthic faunal
53
54 77 communities (Jones, 1971; Ojeda and Santelices, 1984; Dean and Connell, 1987; Smith et al., 1996;
55
56 78 Torres et al., 2015). Habitat complexity has been shown to have a powerful influence on algal
57
58 79 meiofaunal communities, as seaweed of simple structure, with more planar surfaces, attract a lesser
59
60
61
62
63
64
65

80 number of species and in lower abundance (Hicks, 1985). Additionally, it is thought that by creating
81 microhabitats, increased complexity in kelp holdfasts augments the number of niches available,
82 reducing in this way competition, and providing protection from physical stress (Gibbons, 1988).
83 Species that are less dependent on drifting may therefore choose to inhabit the holdfast rather than the
84 frond, in order to benefit from the structure's protection against currents and potential predators
85 (Christie et al., 2007). Furthermore, elevated complexity enhances silt accumulation, which becomes
86 trapped in holdfasts (Moore, 1972). This may explain why both psammic and phytal organisms are
87 found within holdfasts, adding diversity to the specialist fauna already present (Arroyo et al., 2004).
88 Spatial complexity created by holdfast branching may cause competition for hapteron attachment sites
89 and encourage sessile species to occupy voids created between haptera (Moore, 1986). Tubicolous and
90 sessile fauna, like polychaetes, bivalves and sponges, also create habitats for other organisms, which
91 can inhabit vacated tubes and benefit from increased habitable surface (Smith et al., 1996).

92 Despite numerous studies on this topic, the general lack of quantitative ecological data has been
93 highlighted at multiple times (Arroyo et al., 2004; Anderson et al., 2005): the relationship between
94 habitat complexity and biodiversity can neither be fully explained by surface-area alone nor by
95 holdfast weight or volume (Hicks, 1985; Smith et al., 1996; Norderhaug et al., 2002; Arroyo et al.,
96 2004; Hauser et al., 2006; Norderhaug et al., 2007). Current theories on habitat complexity are often
97 based on these variables, and rarely account for other factors that influence the structure. They may
98 thus dismiss important architectural features of the habitat. Additionally, previous studies that have
99 established the importance of structural complexity in explaining patterns of diversity have only
100 addressed this issue using artificial mimics (Hauser et al., 2006; Christie et al., 2007; Norderhaug et
101 al., 2007). The fact that chemicals released by the structure may influence the species which choose to
102 inhabit it (i.e. amount of dissolved oxygen, chemical cues and nutrient flow) and that communities
103 may evolve over time (Bell et al., 1991) should be accounted for.

104 Several methods have been applied in ecology to quantify complexity. Most commonly, the
105 analysis of fractal geometry has been used in marine ecological contexts (Jeffries, 1993; Gee and
106 Warwick, 1994a,b, McAbendroth et al., 2005; Torres et al., 2015). Fractal objects are those whose size
107 increases as their unit of measurement decreases (Mandelbrot, 1967), and fractal geometric patterns

108 are observable in various naturally occurring objects like coastlines, coral reefs and leaf vegetation
109 (Sugihara and May, 1990). The fractal dimension (FD) – the rate by which the object size increases
110 with decreasing units – provides a quantifiable measure of complexity, independent of the nature of
111 the structure, and accounts for habitat scale and what it represents for organisms of different sizes (Gee
112 and Warwick, 1994b). Less explored methods include the use of indices of spatial auto-correlation, i.e.
113 a quantification of the similarity between objects considering the proximity between them, such as
114 Moran’s index and Geary’s coefficient (Legendre and Fortin, 1989; Corrêa da Silva et al., 2008).
115 Similarly to fractal dimensions, spatial autocorrelation methods are multi-dimensional: so long as the
116 factors are weighted correctly, the latter can be applied to three-dimensional spaces, such as kelp
117 (Chen, 2013).

118 The primary aim of the present study was to investigate the relationship between habitat
119 complexity and faunal biodiversity in kelp holdfast communities. The application of a novel method to
120 quantify a complex biological structure is presented. Computer-aided tomography (CT-) scanning is a
121 technique typically applied for medical uses that has more recently been used in an ecological context
122 to portray aspects of 3-dimensional structure and complexity (Mazik et al., 2008; Naumann et al.,
123 2009; Faulwetter et al., 2013). In the present study, CT-scanning was used for the first time to acquire
124 detailed 3D data from holdfasts of the kelp *Laminaria hyperborea* and establish whether structural
125 complexity of holdfasts relates to holdfast fauna community structure. This species of brown alga is an
126 ideal model for studies on habitat complexity due to the intricate and ramified nature of its holdfast as
127 well as its importance as a benthic habitat (Arroyo et al., 2004; Norderhaug et al., 2007; Christie et al.,
128 2007; Blight and Thompson, 2008). By offering 3D imagery of the habitat, CT-scanning enabled *in*
129 *vivo* visualization of both the internal and external rhizoid assemblage – spatial information otherwise
130 difficult to acquire (Dutilleul et al., 2005). Indeed, the main advantage of CT-scanning is that it allows
131 access to quantitative data that are extremely relevant to architectural properties of the habitat (e.g.
132 surface, volume, fractality). The benthic fauna inhabit the holdfast’s surface and internal spaces, and
133 thus the information acquired through this method is a reflection of the provision of substrate for fauna
134 and associated protection from currents and predators. As the kelp holdfasts used in this experiment
135 have geometrical patterns that lend themselves well to fractal analysis, and as the distribution of voxel

136 intensities in the scans is associated to some form of spatial variability (Corrêa da Silva et al., 2008),
137 fractal dimensions and spatial autocorrelation indices were computed from the CT-scan data in order
138 to quantify the spatial complexity of the holdfast habitat. We hypothesized that increased habitat
139 complexity leads to increased faunal biodiversity.

2. Materials and methods

2.1 Sample collection

144 Seventeen individual *Laminaria hyperborea* holdfasts of different sizes (5.19 - 240.42 cm³) were
145 collected sub-tidally by SCUBA divers, at random positions within two kelp beds in the Plymouth
146 Sound, UK: Andurn Point (50°19.235' N, 004°07.820' W) and Ramscliff Point (50°19.558' N,
147 004°07.820' W) on the 22nd of February 2013. Both sites are characterized by a similar degree of wave
148 exposure and water depths (7-11m). The stipe of each individual was cut 5 cm above the holdfast with
149 a diver's knife and each holdfast was levered carefully from the substrate before being placed quickly
150 into a plastic bag, which was immediately sealed with a cable-tie. Great care was taken to avoid
151 damaging the structure of the holdfasts during collection. Each bag containing a holdfast was then
152 placed into another bag to reduce the risk of losing the mobile fauna if the first bag was damaged. To
153 exclude air from entering the holdfast structure, as this could affect CT-scanning results, each bag
154 containing a holdfast was immediately placed in a bucket of seawater on retrieval to the dive boat. The
155 holdfasts were transported in individual buckets to Plymouth Marine Laboratory, UK.

2.2 Pre-scanning procedure

158 During CT-scanning, the absorption of X-rays is sensitive to differences in the density of the materials
159 scanned (Mazik et al., 2008; Ketcham and Carlson, 2011). The CT-value obtained is an average of the
160 properties of the different materials, meaning the material boundaries may be blurred, and leading to
161 what is referred to as partial-volume effects (Ketcham and Carlson, 2011). In order to limit such
162 artifacts, which may affect the resolution of the imagery, as much of the fauna as possible was
163 removed from the holdfasts prior to scanning. The best method to do so in a non-destructive way was

164 sonication. Without removing them from their plastic bags, each holdfast was placed in an ultra-sound
165 bath for 15 min. Once the samples had been sonicated, in order to ensure the holdfasts were immersed
166 at all times and to avoid exposure to air, they were transferred into buckets of locally collected
167 seawater in which the rest of the procedure was carried out. The plastic bags were then cut open and
168 the holdfasts were left to sit for 10 min, to allow fauna to escape. The fauna extracted during this
169 procedure was sieved over a 250 μm mesh and fixed in 10% buffered formaldehyde. Each holdfast
170 was then immersed into the same formaldehyde solution within a standard plastic pot for scanning,
171 with particular care not to introduce air bubbles into the holdfast structure. The pots were selected for
172 their low X-ray absorption levels, to maximize the quality of the scan (Lontoc-Roy et al., 2006). Fauna
173 samples were preserved in 75% industrial methylated spirit after 48 hours until analysis.

2.3 CT-scan data acquisition and post-processing

176 Each holdfast was scanned at the CT Suite of the Radiology Department located at Torbay Hospital, in
177 a helical, medical high resolution CT-scanner (Discovery CT750HD, GE Healthcare). CT-scanning
178 generates two-dimensional cross sectional images called slices using a single x-ray tube and an array
179 of detectors that rotate around the object of study. Reconstructed slices are then used to recreate the 3
180 dimensional structures as a composite (Dufour et al., 2005; Ketcham and Carlson, 2011). The CT-scan
181 configuration parameters were set at 80 kV for the X-ray tube voltage and 300 mA for the X-ray tube
182 current. Rotation speed was set at 0.7 s, the table moved at 15.1 mm/s and exposure time was 10-12 s.
183 The image reconstruction interval was 0.625 mm, giving a voxel size of 0.244 mm^3 (a voxel is a
184 “volume pixel” – a unit of volume in three-dimensional space; the smaller a voxel, the higher the
185 resolution of the image). 2D slice size was 512 x 512 pixels. Images were saved in DICOM format in,
186 16-bits and 3D composites reconstructed using the freeware OsiriX version (Rosset et al., 2004; Fig.
187 1a and b).

188 The raw CT-scan images were transformed into a set of raster files, each one encoding a 2
189 dimensional cut through the object. In other words, the images were stored as a succession of voxels,
190 each of which was specified by its position (x,y,z) and its brightness $I(x,y,z)$, normalized between 0
191 and 1. As the interest hereby lies in extracting geometrical properties of the images, the first step was

192 to segment the image in order to: i) remove the background noise inherent to the CT-scan; and ii)
193 remove the image of the pot housing the kelp. Since the noise and the container correspond to low
194 values of the brightness intensity, a threshold θ was defined such that any intensity lower than θ was
195 set to 0, and any intensity larger was set to 1. By doing so, all the background noise was removed as
196 well as the image of the container and all the significant voxels were set to the maximal brightness 1.
197 Each kelp was hereafter represented by a filtered image, defined by voxels with $I(x,y,z) = 0$ or 1 (Fig.
198 2).

2.4 Processing of fauna and kelp samples

201 Following scanning, the holdfasts were manually broken up and thoroughly washed over a $250 \mu\text{m}$
202 sieve to retain the remaining fauna, which was fixed and preserved as before. All collected individuals
203 were pooled per kelp, and all individuals were counted and identified under low power magnification
204 ($\times 500$), to the lowest taxonomic level possible. Finally, the age of each kelp plant was determined
205 using the method of Kain (1963), which consists of splitting the stipe in half longitudinally just above
206 the holdfast and counting the number of growth rings present. The number of separate haptera
207 branching out from the stipe was also recorded.

2.5 Image analysis and calculation of complexity indices

2.5.1 Volume

212 Calculating the volumes of the holdfast presents an adequate measure of inhabitable space within the
213 kelp. The volumes of the kelps were computed by drawing regions of interest (ROIs) as precisely as
214 possible onto each 2D slice of the scanned holdfast at maximum resolution, using the image software
215 OsiriX. In principle, these measurements could also be obtained by counting the total number of
216 voxels with brightness 1 on the filtered image, and multiplying it by the volume of a voxel $v = a^3$,
217 where a is the spatial resolution of the scanner in the x , y and z direction. Indeed, the filtered encoding
218 of the images allows for the computation of all kind of geometrical properties of the kelp.

220 2.5.2 Surface

1
2 221 Since a number of organisms live on the surface of the kelp, it is interesting to retrieve information
3
4 222 from the scans pertaining to the surface area. Using the filtered data, the surface area was extracted
5
6 223 using two algorithms defining the surface of the kelp:

7
8 224
9
10
11 2251. *Translation*: consider the image of a kelp after threshold. This image can be translated by one voxel in
12
13 226 a given direction (for example the z-direction, perpendicular to the planes of the CT-scan). The voxels
14
15 227 that are different in the original and in the translated image belong to the surface of the kelp (this is
16
17 228 true only after restricting the brightness intensity to 0 or 1).

18
19
20 2292. *Neighbours*: since the image is 3-dimensional, each point of the grid has 6 neighbours. A voxel
21
22 230 belongs to the bulk of the kelp if it has exactly 6 direct neighbours with an equal brightness of 1, and
23
24 231 belongs to its surface if its number of neighbours is smaller than 6.

25
26 232
27
28
29 233 Both methods were tested, and these gave results that were consistent with each other. Throughout this
30
31 234 paper, the surface areas were computed by the translation method. The total surface area of the kelp is
32
33 235 thus equal to the number of voxels of the surface, times the area of a face of the voxel, a^2 .

34
35 236

37 237 2.5.3 Fractal dimension

38
39
40 238 An important characteristic of a complex geometry is its fractal dimension (Mandelbrot, 1983). It
41
42 239 quantifies the degree of branching and embedded small structures of the object. It is defined
43
44 240 mathematically in the following way: given a geometrical object, in order to cover it with voxels of
45
46 241 size ϵ^3 , one needs $N(\epsilon)$ such voxels. When the linear size ϵ gets smaller (i.e. the resolution increases),
47
48
49 242 a larger number of voxels $N(\epsilon)$ is needed to cover the object. The fractal dimension, d_F , characterizes
50
51 243 how the number of voxel increases when the resolution increases and is defined mathematically as the
52
53 244 limit:

$$d_F = - \lim_{\epsilon \rightarrow 0} \frac{\text{Log } N(\epsilon)}{\text{Log } \epsilon}$$

54
55
56
57
58
59 245 where Log denotes the natural logarithm function.

60
61
62
63
64
65

246 The fractal dimension can be computed by using the “box counting” method (Mandelbrot, 1983).
 1
 2 247 Starting at the highest resolution (i.e. smallest voxel size a), a voxel is said to be occupied (by kelp) if
 3
 4 248 its value is 1, otherwise it is said to be empty. The total number $N(a)$ of occupied voxels at this
 5
 6 249 resolution is calculated. Now consider double sized voxels with linear size $2a$. Each of these new
 7
 8 250 voxels comprise $2 \times 2 \times 2 = 8$ smaller original voxels. Each of these is occupied if it contains at least 4
 9
 10
 11 251 occupied smaller voxels, and empty otherwise. The number $N(2a)$ of occupied voxels of size $2a$ can
 12
 13 252 now be computed. This procedure is iterated by doubling the size of the voxels and computing each
 14
 15 253 time the corresponding number of occupied new voxels. A log-log plot of $N(\epsilon)$ as a function of the
 16
 17 254 resolution ϵ can then be plotted. If the object is fractal, this plot is expected to look like a straight line
 18
 19
 20 255 with a negative slope, the slope being the fractal dimension.

21
 22 256 It is interesting to note here the relevance of the fractal dimension of the surface. Indeed, the
 23
 24 257 concept of fractal dimension can be applied to the volume voxels – all the voxels of the image – or to
 25
 26 258 the surface voxels, obtained by either method described above. The small hierarchical structures
 27
 28
 29 259 constituting the surface of the holdfast provide suitable habitats for small organisms, and thus it is
 30
 31 260 logical to try to correlate the biological diversity with the surface fractal dimension of the kelp. The
 32
 33 261 surface fractal dimension of the kelp is calculated by the box-counting method, exactly as depicted
 34
 35 262 previously, except that the voxels used are those of the surface, computed by the translation algorithm
 36
 37
 38 263 described above. According to the above definition, the fractal dimension is just the opposite of the
 39
 40 264 slope of the best-fit straight line. Practically, the fractal dimension was computed by doing a best
 41
 42 265 linear fit for $\log N(\epsilon)$ as a function of $\log \epsilon$, where ϵ takes the value of the resolution at each of five
 43
 44 266 resolutions.

45
 46 267

47 268 2.5.4 Spatial autocorrelation

48
 49 269 Holdfast complexity was also measured using 3D extensions of 2D spatial autocorrelation indices. 3D
 50
 51 270 extensions of the spatial autocorrelation indices were calculated with Moran’s I (Moran, 1950) and
 52
 53
 54 271 Geary’s C (Geary, 1954) using a custom made program in Fortran, based on equations from Marwan
 55
 56
 57 272 et al. (2012) and Corrêa da Silva et al. (2008). The Moran index I and the Geary coefficient C were
 58
 59
 60 273 computed as:

61
 62
 63
 64
 65

$$I = \frac{N}{\sum_i \sum_j \omega_{ij}} \frac{\sum_i \sum_j \omega_{ij} (X_i - \bar{X})(X_j - \bar{X})}{\sum_i (X_i - \bar{X})^2}$$

$$C = \frac{(N - 1)}{2 \sum_i \sum_j \omega_{ij}} \frac{\sum_i \sum_j \omega_{ij} (X_i - X_j)^2}{\sum_i (X_i - \bar{X})^2}$$

where \bar{X} is the mean value of all the voxel values, N is the total number of voxels, X_i is the voxel value at particular point i, X_j is the voxel value at a particular point j ($i \neq j$) and ω_{ij} is the neighbourhood matrix, equal to 1 when i and j are neighbours, and to 0 if else.

2.6 Statistical analysis

Diversity indices capture different aspects of biodiversity, and it is therefore customary to calculate various indices in parallel to capture those different aspects (Magurran, 2004). The total number of species (S), number of individuals – abundance – (N), species richness (Margalef's d), species evenness (Pielou's J) and a diversity index representing a balance between both richness and evenness (Shannon-Wiener's H') were calculated using the faunal abundance data. All possible pairwise correlations between explanatory and response variables were identified by carrying out a Spearman's rank correlation (ρ) test (Fig. 3). All of the 15 possible pairwise correlations between the 6 complexity explanatory variables were significant (Fig. 3). The variable "site" from which the holdfasts were collected was not correlated to any of the explanatory variables (Fig. 3). Since the holdfasts from the two sites did not differ significantly in terms of their age or structural attributes, "site" was not included as a factor in the diversity indices analyses. Univariate measures of community assemblage do not account for the identity of species present and therefore they may be less sensitive than multivariate methods (Warwick and Clarke, 1991). As their output is under numerical form though, they can more directly be related to the indices of complexity developed here (Gee and Warwick, 1994a).

301

1

2 302 2.6.1 Partial least squares regressions

3

4 303 Partial least squares regression analyses (PLSRs) were carried out to quantify how much each of the

5

6 304 explanatory variables (holdfast complexity, i.e. number of haptera per unit volume and fractal

7

8 305 dimension of the surface, as well as kelp age, number of haptera, surface area and volume of the

9

10 306 holdfasts) explained the variance structure of each diversity measure, separately. The PLSR algorithm

11

12 307 finds a reduced number of components (latent variables) maximizing the percentage of variance

13

14 308 structure of a response variable (in this case, each of the diversity indices) explained by the matrix of

15

16 309 potential predictors (i.e. complexity proxies, Carrascal et al., 2009). This method is an extension of

17

18 310 multiple regression methods, and is particularly suited as a tool for small sample sizes and correlated

19

20 311 predictor variables (Carrascal et al., 2009), as is the case here. The correlations between all possible

21

22 312 pairwise correlations suggested a PLSR analysis was appropriate, due to the large number of

23

24 313 correlated explanatory variables and small sample size (i.e. 17 observations (individual holdfasts) and

25

26 314 correlations identified between all predictor variables, Fig. 3). Individual PLSRs were carried out in

27

28 315 order to determine the percentage contribution of holdfast physical attributes and indices of

29

30 316 complexity in explaining the variance structure of each response variable. The PLSR were performed

31

32 317 using the “pls” package (Mevik and Wehrens, 2007) in the open source statistical software R (R Core

33

34 318 Team, 2012).

35

36 319

37

38 320 2.6.2 Multivariate analysis

39

40 321 Multivariate ordination and clustering methods were undertaken to further highlight potential

41

42 322 differences in faunal assemblage structure between kelp holdfasts of varying complexity, using the

43

44 323 statistical analysis software Plymouth Routines In Multivariate Ecological Research 6+ (PRIMER,

45

46 324 Clarke and Gorley, 2006). The species abundance data was 4th-root transformed to down-weight the

47

48 325 influence of heavily abundant taxa (Clarke, 1993) and the rest of the analysis was carried out on both

49

50 326 datasets (hereafter “transformed” and “untransformed data”). Prior to further analysis, the effect of

51

52 327 site on fauna community structure was examined again, as holdfast collection had been carried out at

53

54 328 two different sites. Using the PERMANOVA+ routines add-in to PRIMER 6, a preliminary non-

55

56

57

58

59

60

61

62

63

64

65

329 parametric permutational multivariate analysis of variance (PERMANOVA; Anderson, 2001) was
1
2 330 carried out using “site” as a fixed factor and the community matrix as the response variables. This
3
4 331 analysis showed that although the faunal assemblages differed significantly between sites, no
5
6 332 significant interaction was found between the effect of site and the other independent variables listed
7
8 333 in Table 1 on assemblage structure. This indicated that, despite being different, the kelp holdfast
9
10 334 communities at each site responded similarly to the complexity measures used. As such, “site” was not
11
12 335 considered in the subsequent multivariate analysis. To assess the similarity of the holdfast faunal
13
14 336 communities, a non-metric multidimensional scaling (nMDS) was conducted using the Bray-Curtis
15
16 337 similarity index (Clark and Warwick, 2001). To visualize similarities in assemblages between
17
18 338 holdfasts, an nMDS was plotted in a two-dimensional space preserving the multidimensional distance
19
20 339 between kelp communities based on similarity. Individual communities were labeled on the plot using
21
22 340 circles with a diameter proportional to the values of each explanatory variable (i.e. bubble plot) to
23
24 341 investigate possible similarity between holdfast communities and holdfast complexity attributes.
25
26 342 Finally, a BEST analysis was carried out on the transformed data, to identify which variable, or
27
28 343 combination of variables, best explains the patterns of faunal assemblage similarity (Clarke and
29
30 344 Gorley, 2006).

345 346 **3. Results**

347 348 **3.1 Complexity of holdfasts**

349 3.1.1 Fractal dimension

350 Fractal dimensions of objects embedded in 3-dimensional space are comprised between 0 and 3
351 (Mandelbrot, 1983; Russ, 2013). The values for the fractal dimension of the surface fell within this
352 interval (Table 1). This method is a promising avenue as the use of CT-scanner does allow for a fractal
353 analysis in full 3 dimensions whereas traditional techniques, more commonly described in the
354 literature, are reduced to 2 dimensions.

355 356 3.1.2 Spatial autocorrelation

357 The values for Moran's I and Geary's C fell within their expected values ($I=[-1;1]$, $C=[0;2]$), however
 1
 2 358 they were not correlated to any of the diversity indices and did not seem to be appropriate indicators of
 3
 4 359 complexity in this study. They were therefore not considered further.

6 360

9 361 **3.2 Holdfast communities**

10
 11 362 A total of 7206 individuals from 159 taxa were identified. Juvenile Nereididae (Annelida) was the
 12
 13 363 most numerically dominant group, constituting 23.7% of the total abundance. *Verruca stroemia*
 14
 15 364 (Arthropoda) were also well represented in the assemblages (19% of the total abundance). *Anomioidea*
 16
 17 365 (Mollusca), *Hiatella arctica* (Mollusca), and Nematoda formed another 22.7% of the number of
 18
 19 366 individuals. Polychaete (Annelida) species (67 in total) constituted 42.1% of total species and
 20
 21
 22 367 amphipods another 20.1% with 32 different species.

24 368 The number of species (S) within a holdfast ranged between 18 and 82 and abundance (N) between
 25
 26 369 51 and 1082, thus exhibiting important variations between holdfasts in terms of species richness (d),
 27
 28
 29 370 which ranged between 2.52 and 11.89 (Table 1). Shannon-Wiener's species richness and evenness
 30
 31 371 values were comprised between 0.72 and 3.33 and Pielou's evenness J between 0.21 and 0.90.

33 372 On closer analysis of the raw abundance data, one of the holdfasts (sample 7) exhibited a
 34
 35 373 surprisingly high total number of individuals (N=706, 618 of which are juvenile nereids) compared to
 36
 37 374 its volume (48.27 cm³), haptera.cm⁻³ (0.50) and age (4 years old). As Shannon-Wiener's H' and
 38
 39
 40 375 Pielou's J are indices of diversity that take into account evenness, they are especially sensitive to
 41
 42 376 outliers in the abundance data and are strongly influenced by dominant species. Consequently, this
 43
 44 377 individual holdfast showed very low values for H' (0.72) and J (0.21) (Table 1), indicating low
 45
 46
 47 378 heterogeneity in the assemblage and a highly uneven distribution of species. The correlation plot (Fig.
 48
 49 379 3) confirmed this with strongly skewed graphs and a clear outlier point in both H' and J. Thus, this
 50
 51 380 holdfast was removed in further analyses in order to avoid observing unexpected variance structures in
 52
 53 381 H' and J.

55 382

58 383 **3.3 Statistical analysis**

60 384

61
 62
 63
 64
 65

385 3.3.1 Partial least squares regressions

1
2 386 The loading plots of the PLSR analyses for each response variable revealed that the majority of the
3
4 387 variance structure in each biodiversity index was best explained by components for which volume had
5
6 388 the highest loading among all potential explanatory variables (Fig. 4). However, the contribution of
7
8 389 the other 5 variables for the best component– age, surface area, fractal dimension, haptera number and
9
10
11 390 haptera.cm⁻³ – closely followed that of volume, with approximately equal loading values, indicating
12
13 391 they all played an important role in explaining the variance observed in each response variable
14
15 392 explained by that component.

17 393 The most important findings of the PLSR analyses are presented in Table 2. The same relationships
18
19 394 were observed for S and d, as these indices were strongly correlated to each other (Fig. 3). Despite
20
21
22 395 yielding slightly lower values of variance explained by the PLSR on S, N and d, the variance
23
24 396 structures for both H' and J showed comparable patterns to that of the other biodiversity indices.

26 397 In sum, volume influenced biodiversity the most, followed by age, and the fractal dimension of the
27
28 398 surface (Fig. 4; Table 2). It is interesting to note that the full models with 5 components explained
29
30
31 399 between 37.17% and 81.19% of the variance structure, meaning that other factors not included in this
32
33 400 analysis must account for the remaining variance.

35 401

38 402 3.3.2 Multivariate analysis

39
40 403 The BEST analysis suggested that the combination of surface area and number of haptera per unit of
41
42 404 volume of holdfast explained most of the similarity structure in the community matrix, and this effect
43
44 405 was more evident in the less abundant species (4th root transformed data, $\rho_{\text{Spearman}} = 62.1\%$ and
45
46
47 406 $p < 0.05$) than in the numerically dominant species (untransformed data, $\rho_{\text{Spearman}} = 38.0\%$ and
48
49 407 $p < 0.05$). This pattern was evident in the nMDS plots (Fig. 5), suggesting that number of haptera per
50
51 408 unit of volume (Fig. 5a and c) and surface area (Fig. 5b and d) have opposite effects on community
52
53
54 409 structure. This observation is evidenced by the results from the correlation analysis (Fig. 3): high
55
56 410 surface area coincides with low haptera.cm⁻³, and is negatively correlated to all the other explanatory
57
58 411 variables too.

59
60
61
62
63
64
65

412 The nMDS plots yielded stress values between 0.08 and 0.13, indicating the data were well
1
2 413 represented by the two-dimensional plots and that reliable interpretations could be made from them
3
4 414 (Clarke, 1993).

9 416 4. Discussion

10
11 417
12
13 418 Using indices of complexity that had never been applied in this context previously, the relationship
14
15 419 between habitat complexity and marine biodiversity was demonstrated while investigating structural
16
17 420 features of *Laminaria hyperborea* holdfasts. This study also demonstrated the great potential of CT-
18
19 421 scanning as a tool for ecological studies concerned with habitat complexity, particularly in the study of
20
21 422 kelp systems. The 3D imaging post-processing techniques described here represent a first approach to
22
23 423 examine a quantitative relationship between faunal diversity and kelp holdfast 3D complexity. In
24
25 424 particular, the surface area of the kelp holdfasts could be easily calculated – a measurement otherwise
26
27 425 extremely difficult to obtain – and rarer indices of complexity like fractal dimensions (volume or
28
29 426 surface) and spatial autocorrelation indices could be computed. Albeit frequently overlooked in
30
31 427 ecological studies, partial least squares regression (PLSR) analysis were shown to be an appropriate
32
33 428 and promising statistical tool for spatial analyses like this one, which often require using numerous,
34
35 429 correlated variables (Rossi and Van Halder, 2010) – in this case, by enabling the identification of those
36
37 430 spatial attributes that were most consistently linked to diversity attributes. The PLSR analyses showed
38
39 431 that volume explained the majority of the variance structure observed in all the fauna biodiversity
40
41 432 indices. Community structure was, however, best explained by surface area and haptera per unit
42
43 433 volume of the holdfast.

44
45 434 The fact that volume emerged as the most important explanatory variable agreed with previous
46
47 435 studies (Jones, 1973; Ojeda and Santelices, 1984; Smith et al., 1996; Blight and Thompson 2008;
48
49 436 Torres et al., 2015). Volume constitutes a good measure of the amount of living space available for
50
51 437 organisms; an increase in volume implies there are more niches to colonize, and is likely to reflect also
52
53 438 an increase in resources. Rather than indicating how much living space is available, surface area
54
55 439 reveals how much attachment space is provided for individuals and haptera per unit volume represents
56
57
58
59
60
61
62
63
64
65

440 the amount of inter-haptera space created by the structure. These measures are therefore good indices
1
2 441 of complexity as they account for the multiplicity of microhabitats created by the branching of the
3
4 442 haptera, and these indices were expected to be important drivers of community structure. Our
5
6 443 multivariate analysis revealed this to be true, with different faunal assemblages responding differently
7
8 444 to varying levels of complexity. The fact that less abundant species were more responsive to the effect
9
10
11 445 of surface area and haptera.cm⁻³ than dominant ones could have been expected because these species
12
13 446 will benefit the most from increases in attachment space complexity, whilst dominant species will
14
15 447 occupy the majority of the attachment space available.

17 448 The strong correlation observed between kelp age and volume, surface area, haptera number and
18
19
20 449 haptera.cm⁻³ underlines the importance of determining the age structure of kelp forests in order to
21
22 450 define adequate conservation measures in this type of habitat. Indeed, since knowing the age of kelp
23
24 451 can help estimate its level of complexity, which itself has been shown in the current study to be linked
25
26 452 to biodiversity levels, age should be a determinant factor when restoring previously damaged kelp
27
28
29 453 beds, and when electing which beds to prioritize for management or fishing (Bell et al., 1991).
30
31 454 Additionally, as volume and surface area were negatively correlated to haptera per unit volume, we
32
33 455 hypothesized that as the kelps grows, it adds volume and surface more quickly than it adds new
34
35 456 haptera at the stipe. This would suggest that the complexity of the holdfast arises from the multiplicity
36
37
38 457 of haptera emerging from extant haptera, rather than from the addition of new haptera at the stipe.

40 458 The composition of the faunal communities recorded here is similar to that reported by Moore
41
42 459 (1973), in which Syllidae, Nereididae, Terebellidae, Corophiidae and Ischyroceridae were identified as
43
44 460 the families with the highest abundance in *Laminaria hyperborea* holdfasts. The holdfast is an ideal
45
46 461 environment for amphipods which feed on sediment particles rich in organic matter and for gastropods
47
48
49 462 that graze on the algae or filter-feed passively (Moore, 1973). Numerous juvenile individuals, mainly
50
51 463 from the Nereididae family and the Mollusca, as well as juvenile crabs and ophiuroids, were identified
52
53 464 in the holdfasts. Kelp holdfasts thus seem to provide ideal nursing grounds for benthic organisms. This
54
55
56 465 is not surprising given that holdfasts offer physical protection from waves and predators, and trap
57
58 466 sediment rich in nutrients (Dean and Connell, 1987; Steneck et al., 2002). Similarly to the findings of
59
60 467 Smith et al. (1996) on *Ecklonia radiata* holdfasts, the apparent increased abundance of serpulids (e.g.
61
62
63
64
65

468 *Spirobranchus* species) and barnacles in holdfasts of higher complexity may further facilitate increase
1
2 469 in other species (e.g. syllids), which are able to colonize empty calcareous tubes provided by these
3
4 470 organisms.

6 471 Further investigation of the links between taxonomic groups, dispersal modes and feeding
7
8 472 strategies with complexity of the holdfast might shed light on the dynamics of colonization and
9
10 473 community succession in this habitat (Smith et al., 1996). A number of holdfasts investigated here
11
12 474 exhibited particularly high abundance of certain taxa – for instance, hundreds of juvenile nereids but
13
14 475 much fewer other species of polychaetes. This finding may be indicative of founder effects, by which
15
16 476 the multiplication and predominance of certain species of early colonizers is facilitated. Since a large
17
18 477 number of species were found in both simple and complex holdfasts, yet more complex holdfasts
19
20 478 hosted a larger number of species, it is reasonable to suggest that succession occurred through the
21
22 479 addition of species over time rather than species replacement, as suggested by Smith et al. (1996) and
23
24 480 Ojeda and Santelices (1984).

28 481 The CT-scanning data significantly improved our ability to quantify habitat complexity in this
29
30 482 study, and to predict changes in biodiversity with spatial heterogeneity. The usefulness of CT data was
31
32 483 clearly maximized by the computation of otherwise unavailable, or very hardly achievable
33
34 484 measurements. Indeed, surface area and the fractal dimension of the surface are both strongly
35
36 485 positively correlated to species richness, abundance and diversity, and together contribute to about
37
38 486 20% of the variance structure observed in the response variables. Both spatial autocorrelation
39
40 487 coefficients showed high positive autocorrelation within holdfasts and very little variance between
41
42 488 holdfasts of differing size, suggesting the existence of a “typical” holdfasts structure, that was fairly
43
44 489 homogenous between individuals, with low variation at a global and local level. Unfortunately, these
45
46 490 values could not provide explanation towards the biological diversity investigated, and are possible not
47
48 491 promising avenues for future studies with aims similar to ours. Conversely, fractal dimensions gave
49
50 492 biologically meaningful information. By providing an interpretation of habitat size in relation to the
51
52 493 scale of measurement, these measures have also been found to be good predictors of body size in
53
54 494 fauna assemblages in other studies (Gee and Warwick, 1994a,b). While larger volumes may provide
55
56 495 more occasions to find resources and partners to mate with, more fractal surfaces suggest more
57
58
59
60
61
62
63
64
65

496 opportunities to avoid stress and predators, through increased intricacy and hiding areas. The fact that
1
2 497 the biodiversity hereby responded to the surface fractal dimension of the holdfasts suggests that this
3
4 498 variable has ecological implications in benthic communities. Additionally, a study on coralline algal
5
6 499 turf gastropod assemblages found that there may exist an upper threshold of habitat complexity
7
8 500 beyond which species diversity does not increase (Kelaher, 2003). Reduced interstitial space
9
10 501 associated with architecturally more complex habitats, leading to decreased amount of light, food and
11
12 502 space available for organisms, may be particularly important for larger sized fauna, and there may be
13
14 503 an optimal level between the provision of attachment space for fauna, and the complexity of that
15
16 504 habitat space.
17

18
19
20 505 A future avenue that deserves attention should be to fully develop the potential of data extracted
21
22 506 from CT-scanning. A method that could provide additional insightful information in terms of faunal
23
24 507 diversity appears to be the one described by Mazik et al. (2008). In their study of scanned sediment
25
26 508 cores, they extracted information on the burrow volumes and surface areas, as well as on the mean
27
28 509 burrow diameter, mean number of burrows and mean density. It would be interesting to obtain similar
29
30 510 data on the 3D geometry of inter-haptera space, as this would provide a robust measure of the
31
32 511 properties of the holdfast and of the amount of living space available for the fauna (i.e. volumes of the
33
34 512 spaces created by the structure, mean number of spaces and their dimensions which relate to the
35
36 513 probability of having a certain number of spaces of a certain size). Such parameters could provide
37
38 514 another set of indices of complexity, and could be linked more directly to body size distribution of the
39
40 515 fauna, offering considerably more information than that available without scanning. Marwan et al.
41
42 516 (2009; 2012) investigated structural complexity using CT-scanning in a medical context and
43
44 517 developed a method of differentiating shapes with the same volume but different surface areas. In the
45
46 518 present study, quantifying the shapes of the inter-haptera spaces, as well as the variety of these shapes
47
48 519 in relation to the volume, could supplement the analysis well, by providing data relatable to the
49
50 520 morphological diversity of the faunal samples.
51

52
53 521 Despite explaining up to 81% of the variance structure observed, the complexity measures
54
55 522 investigated did not fully explain the variance structure observed in the biodiversity indices, with
56
57 523 lowest correspondence between complexity and community evenness. This finding would suggest that
58
59
60
61
62
63
64
65

524 dominance of holdfast communities is not related to holdfast structural complexity. Future work could
1
2 525 also investigate measurements of complexity in the faunal community that were not used here. For
3
4 526 instance, recording the biomass and size of the faunal samples should provide precious information on
5
6 527 the type of fauna expected to be found in habitats of a certain complexity, as suggested by Warwick
7
8
9 528 and Clarke (1984), who showed that specific traits in animals, and more precisely in benthic fauna,
10
11 529 can be favoured according to their body size. The presence of epiphytes on the stipe of the kelp was
12
13 530 not recorded but numerous studies have previously shown it had a negligible effect on the faunal
14
15 531 community in the holdfast (Dean and Connell, 1987; Norderhaug, 2002; Hauser et al., 2006).

17 532 Interestingly, encrusting organisms were easily identified on the scanned images. Indeed, due to the
18
19
20 533 distinct density of fauna shells and skeletons, one could localize organisms like echinoderms and
21
22 534 sessile mollusks on the holdfast scans alone. Such data could prove to be particularly interesting in the
23
24 535 frame of ocean acidification, a chemical process by which the reduction in pH and consequent
25
26 536 decrease in carbonate ions strongly diminishes the ability for organisms to sustain carbonated
27
28
29 537 skeletons (Fabry et al., 2008). Recent research has already begun to make use of this approach
30
31 538 (Queirós et al., 2015), and the present study shows that this could be extended to kelp holdfast
32
33 539 communities.

35 540 In conclusion, there are many promising extensions for the techniques and approaches presented
36
37
38 541 here. Understanding community structure in keystone habitats such as kelp forests will be critical
39
40 542 when trying to preserve and restore ecosystems and their associated ecological processes (Steneck et
41
42 543 al., 2002). Through the modulation of resources and their strong interactions with faunal communities,
43
44 544 the loss of ecosystem engineers like kelp, can have cascading effects on biodiversity (Coleman and
45
46
47 545 Williams, 2002; Hastings et al., 2007). By reducing the amount of time that would otherwise be
48
49 546 needed to manually slice kelp holdfasts, and by providing information of much higher resolution, CT-
50
51 547 scanning offers a rapid and powerful technique for faunal community monitoring (Mazik et al., 2008)
52
53 548 and a suitable way to assess anthropogenic impacts on macrophyte systems. In particular, it allows
54
55
56 549 detailed visualization of complex systems in their natural state and with minimal disturbance (Dufour
57
58 550 et al., 2005), an impossible task when using artificial structures as proxies of holdfast complexity.
59
60 551 Indeed, it makes it feasible to study kelp populations that have matured over time, which is
61
62
63
64
65

552 particularly meaningful in perennial species. It also accounts for the chemicals released by the kelp,
 1
 2 553 some of which are responsible for the growth of biofilm which facilitate faunal attachment (Hellio et
 3
 4 554 al., 2000), and others which influence the nutritional value of the kelp (Norderhaug et al., 2003; Toth
 5
 6 555 et al., 2005). Importantly, it is the only way to estimate the holdfast surface area precisely. Therefore,
 7
 8 556 CT-scanning provides highly valuable information, and emerges as a unique tool to analyze habitat
 9
 10
 11 557 complexity. Further research could focus on the use of higher resolution devices, improving the extant
 12
 13 558 methods of calculating complexity and developing new ones. The scanning procedure developed here
 14
 15 559 will undeniably prove useful in future ecological research, by providing valuable data for conservation
 16
 17 560 purposes, though the identification of structurally complex communities as biodiversity hotspots,
 18
 19 561 which can help to support efficient design of marine protected areas. Appreciating how the spatial
 20
 21 562 distribution of organisms relates to structural complexity of habitats has great relevance in ecological
 22
 23 563 modeling and can support the projection of the potential consequences of environmental change for
 24
 25 564 the benthos (Tilman, 1994).

26
 27 565
 28
 29 566 **Acknowledgments.** This study was partly funded by the University of Plymouth as part of CO's master's thesis.
 30
 31 567 We thank Sarah Dashfield, Joana Nunes, and Thomas Vance for assistance in the laboratory; Roger Crook and
 32
 33 568 members of the Plymouth University Dive and Marine Center for support with fieldwork; as well as J.H. for help
 34
 35 569 with the computer programming. This paper is a contribution to the Plymouth Marine Laboratory science area
 36
 37 570 "Marine Ecology and Biodiversity". AMQ acknowledges support by the UK Natural Environment Research
 38
 39 571 Council and UK Department for Environment, Food and Rural Affairs (grant number NE/L003279/1, Marine
 40
 41 572 Ecosystems Research Programme).

42
 43 573
 44
 45 574 **References**

- 46
 47 575
 48
 49 576 Anderson, M.J., 2001. A new method for non-parametric multivariate analysis of variance. *Austral. Ecol.* 26,
 50
 51 577 32–46.
 52
 53 578 Anderson, M.J., Connell, S.D., Gillanders, B.M., Diebel, C.E., Blom, W.M., Saunders, J.E., Landers, T.J., 2005.
 54
 55 579 Relationships between taxonomic resolution and spatial scales of multivariate variation. *J. Anim. Ecol.* 74,
 56
 57 580 636–646.
 58
 59
 60
 61
 62
 63
 64
 65

- 581 Arroyo, N.L., Maldonado, M., Pérez-Portela, R., Benito, J., 2004. Distribution patterns of meiofauna associated
1 with a sublittoral *Laminaria* bed in the Cantabrian Sea (north-eastern Atlantic). *Mar. Biol.* 144, 231–242.
2 582
- 3
4 583 Bell, S.S., McCoy, E.D., Mushinsky, H.R., 1991. Habitat structure: the physical arrangement of objects in space.
5
6 584 Chapman and Hall, London
- 7
8 585 Blight, A.J., Thompson, R.C., 2008. Epibiont species richness varies between holdfasts of a northern and a
9
10 586 southerly distributed kelp species. *J. Mar. Biol. Assoc. UK* 88, 469–475.
- 11
12 587 Carrascal, L.M., Galvan, I., Gordo, O., 2009. Partial least squares regression as an alternative to current
13
14 588 regression methods used in ecology. *Oikos* 118, 681–690.
- 15
16 589 Chen, Y., 2013. New approaches for calculating Moran’s index of spatial autocorrelation. *PloS One* 8:e68336.
- 17
18 590 Christie, H., Jørgensen, N.M., Norderhaug, K.M., Waage-Nielsen, E., 2003. Species distribution and habitat
19
20 591 exploitation of fauna associated with kelp (*Laminaria hyperborea*) along the Norwegian Coast. *J. Mar. Biol.*
21
22 592 *Assoc. UK* 83, 687–699.
- 23
24 593 Christie, H., Jørgensen, N.M., Norderhaug, K.M., 2007. Bushy or smooth, high or low; importance of habitat
25
26 594 architecture and vertical position for distribution of fauna on kelp. *J. Sea. Res.* 58, 198–208.
- 27
28 595 Clarke, K.R., 1993. Non-parametric multivariate analyses of changes in community structure. *Aust. J. Ecol.* 18,
29
30 596 117–143.
- 31
32 597 Clarke, K.R., Warwick R.M., 2001. An approach to statistical analysis and interpretation. *Change in Marine*
33
34 598 *Communities* 2.
- 35
36 599 Clarke K.R., Gorley, R.N., 2006. *PRIMER v6: User Manual/Tutorial*. PRIMER-E, Plymouth.
- 37
38 600 Coleman F.C., Williams S.L., 2002. Overexploiting marine ecosystem engineers: potential consequences for
39
40 601 biodiversity. *Trends Ecol. Evol.*, 17, 40–43.
- 41
42 602 Connor E.F., McCoy E.D., 1979. The statistics and biology of the species-area relationship. *Am. Nat.* 113, 791-
43
44 603 833.
- 45
46 604 Corrêa da Silva, E., Corrêa Silva, A., Cardoso de Paiva, A., Nunes, R.A., 2008. Diagnosis of lung nodules using
47
48 605 Moran’s index and Geary’s coefficient in computerized tomography images. *Pattern Anal. Applic.* 11, 89–99.
- 49
50 606 Dean, R.L., Connell, J.H., 1987. Marine invertebrates in an algal succession. III. Mechanisms linking habitat
51
52 607 complexity with diversity. *J. Exp. Mar. Biol. Ecol.*, 109, 249–273.
- 53
54 608 Dufour, S.C., Desrosiers, G., Long, B., Lajeunesse, P., Gagnoud, M., Labrie, J., Archambault, P., Stora, G.,
55
56 609 2005. A new method for three-dimensional visualization and quantification of biogenic structures in aquatic
57
58 610 sediments using axial tomodensitometry. *Limnol. Oceanogr. Meth.* 3, 372–380.
59
60
61
62
63
64
65

- 611 Dutilleul, P., Lontoc-Roy, M., Prasher, S.O., 2005. Branching out with a CT scanner. *Trends Plant Sci.* 10, 411-
1 412.
2
- 3
4 613 Estes, J.A., Tinker, T., Williams, T.M., Doak, D.F., 1998. Killer whale predation on sea otters linking oceanic
5 and nearshore ecosystems. *Science* 282, 473-476.
6 614
- 7
8 615 Fabry, V.J., Seibel, B.A., Feely, R.A., Orr, J.C., 2008. Impacts of ocean acidification on marine fauna and
9 ecosystem processes. *ICES J. Mar. Sci.* 65, 414–432.
10 616
- 11
12 617 Faulwetter, S., Vasileiadou, A., Kouratoras, M., Dailianis, T., Arvanitidis, C., 2013. Micro-computed
13 tomography: Introducing new dimensions to taxonomy. *ZooKeys* 263, 1-45.
14 618
- 15
16 619 Geary, R.C., 1954. The contiguity ratio and statistical mapping. *The Incorporated Statistician* 5, 115-145.
17
- 18 620 Gee, J.M., Warwick, R.M., 1994a. Metazoan community structure in relation to the fractal dimensions of marine
19 macroalgae. *Mar. Ecol. Prog. Ser.* 103, 141-150.
20 621
- 21
22 622 Gee, J.M., Warwick, R.M., 1994b. Body-size distribution in a marine metazoan community and the fractal
23 dimension of macroalgae. *J. Exp. Mar. Biol. Ecol.* 178, 247-259.
24 623
- 25
26 624 Gibbons, M.J., 1988. The impact of sediment accumulations, relative habitat complexity and elevation on rocky
27 shore meiofauna. *J. Exp. Mar. Biol. Ecol.* 122, 225–241.
28 625
- 29
30 626 Hastings, A., Byers, J.E., Crooks, J.A., Cuddington, K., Jones, C.G., Lambrinos, J.G., Talley, T.S., Wilson,
31 W.G., 2007. Ecosystem engineering in space and time. *Ecol. Lett.* 10, 153-164.
32 627
- 33
34 628 Hauser, A., Attrill, M.J., Cotton, P.A., 2006. Effects of habitat complexity on the diversity and abundance of
35 macrofauna colonising artificial kelp holdfasts. *Mar. Ecol. Prog. Ser.* 325, 93–100.
36 629
- 37
38 630 Hellio, C., Bremer, G., Pons, A.M., Le Gal, Y., Bourgougnon, N., 2000. Inhibition of the development of
39 microorganisms (bacteria and fungi) by extracts of marine algae from Brittany, France. *Appl. Microbiol.*
40 631
41
42 632 *Biot.* 54, 543-549.
43
- 44 633 Hicks, G.R.F., 1985. Meiofauna associated with rocky shore algae. In: Moore PG, Seed R (eds) *Ecology of*
45 rocky coasts. Hodder and Stoughton, London, pp. 36-56.
46 634
- 47
48 635 Jeffries, M., 1993. Colonization of artificial pondweeds of differing fractal dimension. *Oikos* 67, 142-148.
49
- 50 636 Jones, C.G., Lawton, J.H., Shachak, M., 1994. Organisms as ecosystem engineers. *Oikos* 69, 373–386.
51
- 52 637 Jones, C.G., Lawton, J.H., Shachak, M., 1997. Positive and negative effects of organisms as physical ecosystem
53 engineers. *Ecology* 78, 1946-1957.
54 638
- 55
56 639 Jones, D.J., 1971. Ecological studies on macroinvertebrate populations associated with polluted kelp forests in
57 the North Sea. *Helgoland Mar. Res.* 22, 417-441.
58 640
59
60
61
62
63
64
65

- 641 Jones, D.J., 1973. Variation in the trophic structure and species composition of some invertebrate communities
1
2 642 in polluted kelp forests in the North Sea. *Mar. Biol.* 20, 351-365.
- 3
4 643 Kain, J.M., 1963. Aspects of the biology of *Laminaria hyperborea*. II. Age, weight and length. *J. Mar. Biol.*
5
6 644 *Assoc. UK* 43, 129-151.
- 7
8 645 Kelaher, B.P., 2003. Changes in habitat complexity negatively affect diverse gastropod assemblages in coralline
9
10 646 algal turf. *Oecologia* 135, 431-441.
- 11
12 647 Ketcham, R.A., Carlson, W.D., 2001. Acquisition, optimization and interpretation of X-ray computed
13
14 648 tomographic imagery: applications to the geosciences. *Comput. Geosci.* 27, 381-400.
- 15
16 649 Legendre, P., Fortin, M.J., 1989. Spatial pattern and ecological analysis. *Vegetatio* 80, 107-138.
- 17
18 650 Lontoc-Roy, M., Dutilleul, P., Prasher, S.O., Han, L., Brouillet, T., Smith, D.L., 2006. Advances in the
19
20 651 acquisition and analysis of CT scan data to isolate a crop root system from the soil medium and quantify root
21
22 652 system complexity in 3-D space. *Geoderma* 137, 231-241.
- 23
24 653 MacArthur, R.H., Wilson, E.O., 1967. The theory of island biogeography. Princeton University Press, Princeton,
25
26 654 NJ.
- 27
28 655 Magurran, A.E., 2004. Measuring biological diversity. Blackwell Science Ltd., Oxford.
- 29
30 656 Mandelbrot, B.B., 1967. How long is the coast of Britain. *Science*, 156:636-638.
- 31
32 657 Mandelbrot, B.B., 1983. The fractal geometry of nature. Freeman, New York, NY.
- 33
34 658 Marwan, N., Kurths, J., Thomsen, J.S., Felsenberg, D., Saporin, P., 2009. Three-dimensional quantification of
35
36 659 structures in trabecular bone using measures of complexity. *Phys. Rev. E* 79: 021903.
- 37
38 660 Marwan, N., Beller, G., Felsenberg, D., Saporin, P., Kurths, J., 2012. Quantifying changes in the spatial structure
39
40 661 of trabecular bone. *Int. J. Bifurc. Chaos* 22, 1250027.
- 41
42 662 Mazik, K., Curtis, N., Fagan, M.J., Taft, S., Elliott, M., 2008. Accurate quantification of the influence of benthic
43
44 663 macro- and meio-fauna on the geometric properties of estuarine muds by micro computer tomography. *J.*
45
46 664 *Exp. Mar. Bio. Ecol.* 354, 192-201.
- 47
48 665 McAbendroth, L., Ramsay, P.M., Foggo, A., Rundle, S.D., Bilton, D.T., 2005. Does macrophyte fractal
49
50 666 complexity drive invertebrate diversity, biomass and body size distributions? *Oikos* 111, 279-290.
- 51
52 667 Mevik, B.H., Wehrens, R., 2007. The pls package: principal component and partial least squares regression in R.
53
54 668 *J. Stat. Softw.* 18, 1-24.
- 55
56 669 Moran, P.A.P., 1950. Notes on continuous stochastic phenomena. *Biometrika* 37, 17-23.
- 57
58
59
60
61
62
63
64
65

- 670 Moore, P.G., 1972. Particulate matter in the sublittoral zone of an exposed coast and its ecological significance
1 with special reference to the fauna inhabiting kelp holdfasts. *J. Exp. Mar. Biol. Ecol.* 10, 59–80.
2 671
- 3
4 672 Moore, P.G., 1973. The kelp fauna of northeast Britain. I. Function of the physical environment. *J. Exp. Mar.*
5
6 673 *Biol. Ecol.* 13, 97-125.
- 7
8 674 Moore, P.G., 1986. Levels of heterogeneity and the amphipod fauna of kelp holdfasts. In: Moore PG, Seed R
9
10 675 (eds) *Ecology of rocky coasts*. Hodder and Stoughton, London, pp. 274-289.
- 11
12 676 Naumann, M.S., Niggli, W., Laforsch, C., Glaser, C., Wild, C., 2009. Coral surface area quantification-evaluation
13
14 677 of established techniques by comparison with computer tomography. *Coral Reefs* 28, 109-117.
- 15
16 678 Norderhaug, K.M., Christie, H., Rinde, E., 2002. Colonisation of kelp imitations by epiphyte and holdfast fauna;
17
18 679 a study of mobility patterns. *Mar. Biol.* 141, 965–973.
- 19
20 680 Norderhaug, K.M., Fredriksen, S., Nygaard, K., 2003. Trophic importance of *Laminaria hyperborea* to kelp
21
22 681 forest consumers and the importance of bacterial degradation to food quality. *Mar Ecol Prog Ser* 255:135-144
- 23
24 682 Norderhaug, K.M., Christie, H., Fredriksen, S., 2007. Is habitat size an important factor for faunal abundances on
25
26 683 kelp (*Laminaria hyperborea*)? *J. Sea Res.* 58, 120–124.
- 27
28 684 Ojeda, F.P., Santelices, B., 1984. Invertebrate communities in holdfasts of the kelp *Macrocystis pyrifera* from
29
30 685 southern Chile. *Mar. Ecol. Prog. Ser.* 16, 65–73.
- 31
32 686 Queirós, A.M., Fernandes, J.A., Faulwetter, S., Nunes, J., Rastrick, S.P.S., Mieszkowska, N., Artioli, Y., Yool, A.,
33
34 687 Calosi, P., Arvanitidis, C., Findlay, H.S., Barange, M., Cheung, W.W.L., Widdicombe, S., 2015. Scaling up
35
36 688 experimental ocean acidification and warming research: from individuals to the ecosystem. *Glob.*
37
38 689 *Change Biol.* 21, 130-143.
- 39
40 690 R Core Team, 2012. R: A language and environment for statistical computing. R Foundation for Statistical
41
42 691 Computing, Vienna, Austria.
- 43
44 692 Rosset, A., Spadola, L., Ratib, O., 2004. OsiriX: An open-source software for navigating in multidimensional
45
46 693 DICOM images. *J. Digit Imaging* 17, 205-216.
- 47
48 694 Rossi, J.P., Van Halder, I., 2010. Towards indicators of butterfly biodiversity based on a multiscale landscape
49
50 695 description. *Ecol. Indic* 10, 452-458.
- 51
52 696 Russ, J.C., 2013. *Fractal surfaces*. Springer Science and Business Media.
- 53
54 697 Simpson, E.H., 1949. Measurement of diversity. *Nature* 163, 688-690.
55
56
57
58
59
60
61
62
63
64
65

- 698 Smith, S.D.A., Simpson, R.D., Cairns, S.C., 1996. The macrofaunal community of *Ecklonia radiata* holdfasts :
1
2 699 Description of the faunal assemblage and variation associated with differences in holdfast volume. Aust. J.
3
4 700 Ecol. 21, 81–95.
- 5
6 701 Steneck, R.S., Graham, M.H., Bourque, B.J., Corbett, D., Erlandson, J.M., Estes, J.A., Tegner, M.J., 2002. Kelp
7
8 702 forest ecosystems: biodiversity, stability, resilience and future. Environ. Conserv. 29, 436–459.
- 9
10 703 Sugihara, G., May R.M., 1990. Applications of fractals in ecology. Trends Ecol. Evol. 5, 79-86.
- 11
12 704 Tews, J., Brose, U., Grimm, V., Tielbörger, K., Wichmann, M.C., Schwager, M., Jeltsch, F., 2004. Animal
13
14 705 species diversity driven by habitat heterogeneity/diversity: the importance of keystone structures. J.
15
16 706 Biogeogr. 31, 79–92.
- 17
18 707 Tilman. D., 1994. Competition and biodiversity in spatially structured habitats. Ecology 75, 2–16.
- 19
20 708 Torres, A.C., Veiga, P., Rubal, M., Sousa-Pinto I., 2015. The role of macroalgal morphology in driving its
21
22 709 epifaunal assemblages. J. Exp. Mar. Biol. Ecol. 464, 96-106.
- 23
24 710 Toth, G.B., Langhamer, O., Pavia, H., 2005. Inducible and constitutive defenses of valuable seaweed tissues:
25
26 711 consequences for herbivore fitness. Ecology 86, 612-618.
- 27
28 712 Warwick, R.M., Clarke, KR., 1991. A comparison of some methods for analyzing changes in benthic community
29
30 713 structure. J. Mar. Biol. Assoc. UK 71, 225-244.
- 31
32 714 Warwick, R.M., Clarke, ,K.R., 1984. Species size distributions in marine benthic communities. Oecologia 61,
33
34 715 32-41.
- 35
36 716 Wright, J.P., Jones, C.G., 2006. The concept of organisms as ecosystem engineers ten years on: progress,
37
38 717 limitations, and challenges. Bioscience 56, 203-209.
- 39
40
41
42
43
44
45
46
47
48
49
50
51
52
53
54
55
56
57
58
59
60
61
62
63
64
65

Table 1 Summary of data, including holdfast number, age, volume, surface area, haptera number, indices of complexity (haptera.cm⁻³, fractal dimension,) and biodiversity indices (S – number of species, N – abundance, d – Margalef’s species richness, H’ – Shannon-Wiener’s species evenness and richness, J – Pielou’s species evenness).

Holdfast	Number					Fractal					
	Age (years)	Surface (cm ²)	Volume (cm ³)	of haptera	Haptera per cm ³	dimension of surface	S	N	d	J	H’
1	2	25.99	10.01	18	1.80	1.89	13	116	2.52	0.77	1.98
2	4	90.81	32.94	21	0.64	1.93	22	125	4.35	0.73	2.25
3	4	43.84	16.44	20	1.22	2.01	22	74	4.88	0.78	2.42
4	5	99.22	18.76	22	1.17	1.69	20	113	4.02	0.79	2.36
5	7	224.23	105.82	22	0.21	1.98	43	240	7.66	0.74	2.76
6	7	104.46	35.36	26	0.74	1.92	27	184	4.99	0.65	2.15
7	4	108.09	48.27	24	0.50	1.96	31	706	4.57	0.21	0.72
8	7	252.42	118.89	32	0.27	1.94	54	275	9.44	0.83	3.33
9	5	95.11	41.81	22	0.53	2.05	18	51	4.32	0.86	2.48
10	6	473.39	201.10	39	0.19	2.04	48	269	8.40	0.79	3.05
11	6	322.49	110.97	30	0.27	2.08	49	437	7.90	0.78	3.04
12	5	256.32	98.72	22	0.22	2.02	62	734	9.25	0.62	2.54
13	5	344.40	132.46	32	0.24	2.08	67	1082	9.45	0.53	2.23
14	5	196.18	72.91	28	0.38	2.02	45	543	6.99	0.61	2.32
15	1	22.60	11.41	11	0.96	1.84	24	74	5.34	0.85	2.70
16	5	329.36	137.78	24	0.17	2.02	53	437	8.55	0.76	2.30
17	1	58.32	5.20	12	2.31	1.72	19	53	4.53	0.90	2.65

Table 2 Percentage of the variance of each response variable explained by each partial least squares analyses component (numbers) given with the associated explanatory variable (volume, haptera number, age, haptera.cm⁻³, surface area and the fractal dimension of the surface) which had the highest loading for that component.

	S	N	d	H'	J
Volume	68.52	38.51	69.34	26.14	20.95
Haptera Number	0.34	4.79	N/A	4.03	5.08
Age	7.81	7.96	9.91	1.13	N/A
Haptera.cm⁻³	N/A	N/A	1.92	2.28	2.64
Surface area	0.94	N/A	N/A	N/A	N/A
FD Surface	1.36	5.83	0.02	17.18	5.58
Variance explained	78.97	58.55	81.19	50.76	37.17

1
2
3
4
5
6
7
8
9
10
11
12
13
14
15
16
17
18
19
20
21
22
23
24
25
26
27
28
29
30
31
32
33
34
35
36
37
38
39
40
41
42
43
44
45
46
47
48
49
50
51
52
53
54
55
56
57
58
59
60
61
62
63
64
65

1
2
3
4
5
6
7
8
9
10
11
12
13
14
15
16
17
18
19
20
21
22
23
24
25
26
27
28
29
30
31
32
33
34
35
36
37
38
39
40
41
42
43
44
45
46
47
48
49
50
51
52
53
54
55
56
57
58
59
60
61
62
63
64
65

Fig. 1 3D reconstruction of a scanned kelp using OsiriX (using a blood-vessel and bone mask to aid visualization - red-brown: kelp; white-gray: calcifying fauna). A) Lateral view of the holdfast. B) View of the base of the holdfast where calcifying fauna can be seen in white, exhibiting densities similar to human bone.

Fig. 2 A) One of the 141 slices constituting the outcome of the CT-scanning of an individual kelp holdfast. B) The similar slice following the cropping of the stipe and bucket after setting a threshold θ . Only the holdfast remains. Non-black voxels were considered as the foreground; black voxels were considered as background and therefore excluded from the surface and fractal dimension calculations.

Fig. 3 Correlations between the variables used in the statistical analysis (both explanatory and response variables). The pie charts depict the strength of the correlations between variables, solid pies indicating a positive correlation and striped pies indicating a negative correlation.

Fig. 4 Loading plots showing the loading value of each variable for the first three main components (values written inside each graph, see table 2 for the percentage contribution of each component). Variables: 1 = surface area, 2 = FD of surface, 3 = age, 4 = number of haptera, 5 = volume, 6 = haptera.cm⁻³.

Fig. 5 Two-dimensional nMDS ordination (Bray-Curtis similarity index) on holdfast assemblages (N=17), after transformation (A and B) and before transformation (C and D), on haptera per unit volume (A and C) and on surface area (B and D).

Figure 1
[Click here to download high resolution image](#)

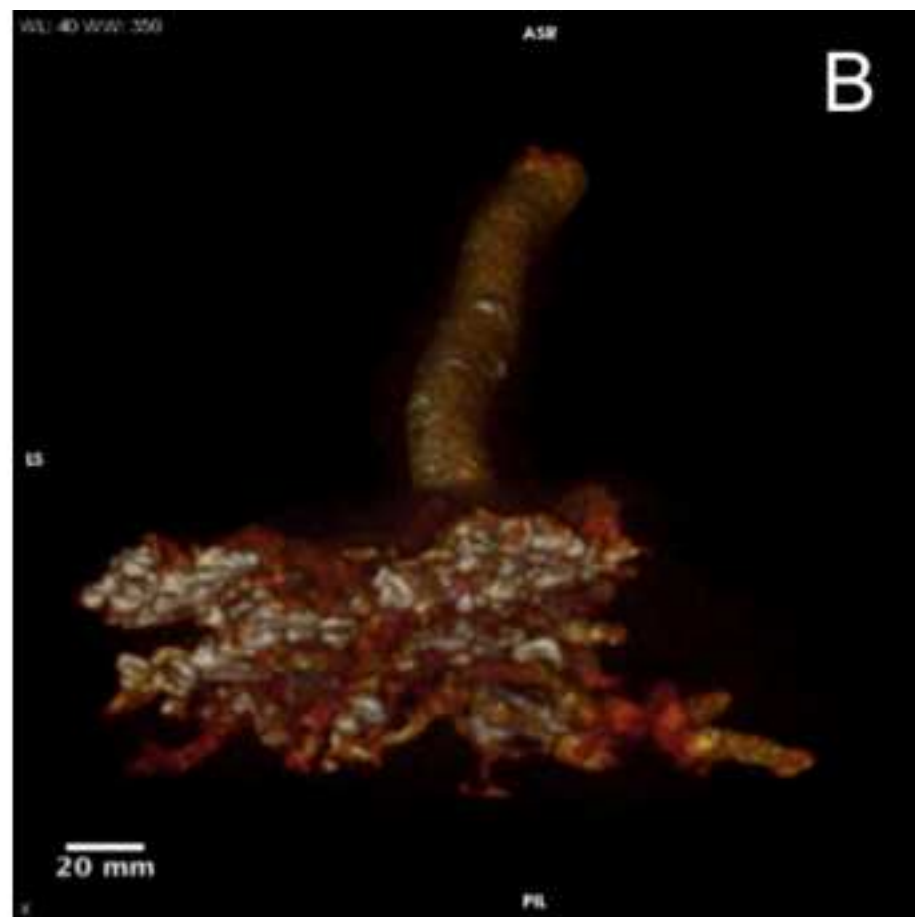
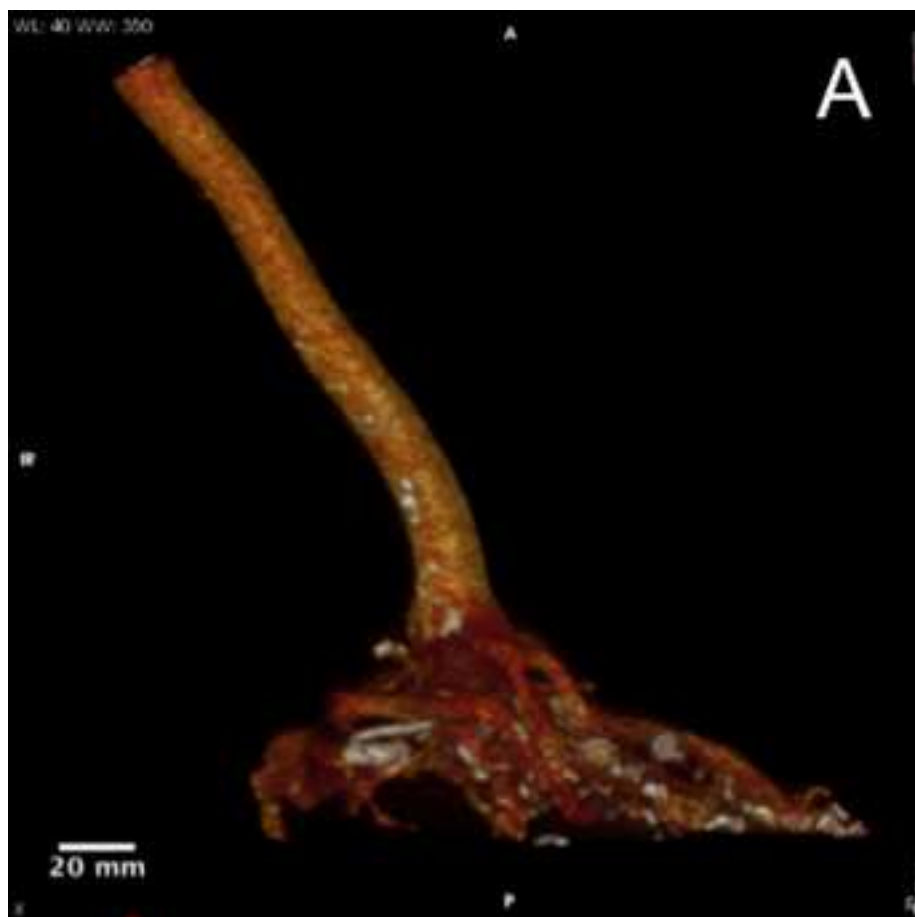


Figure 2
[Click here to download high resolution image](#)

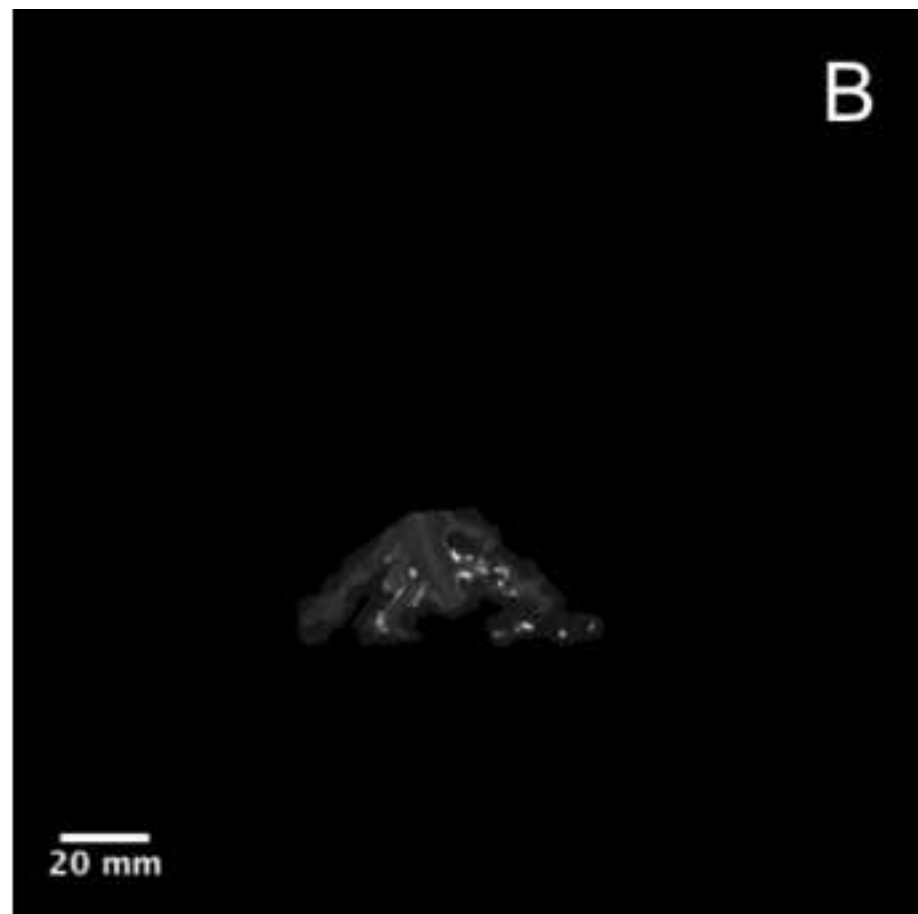
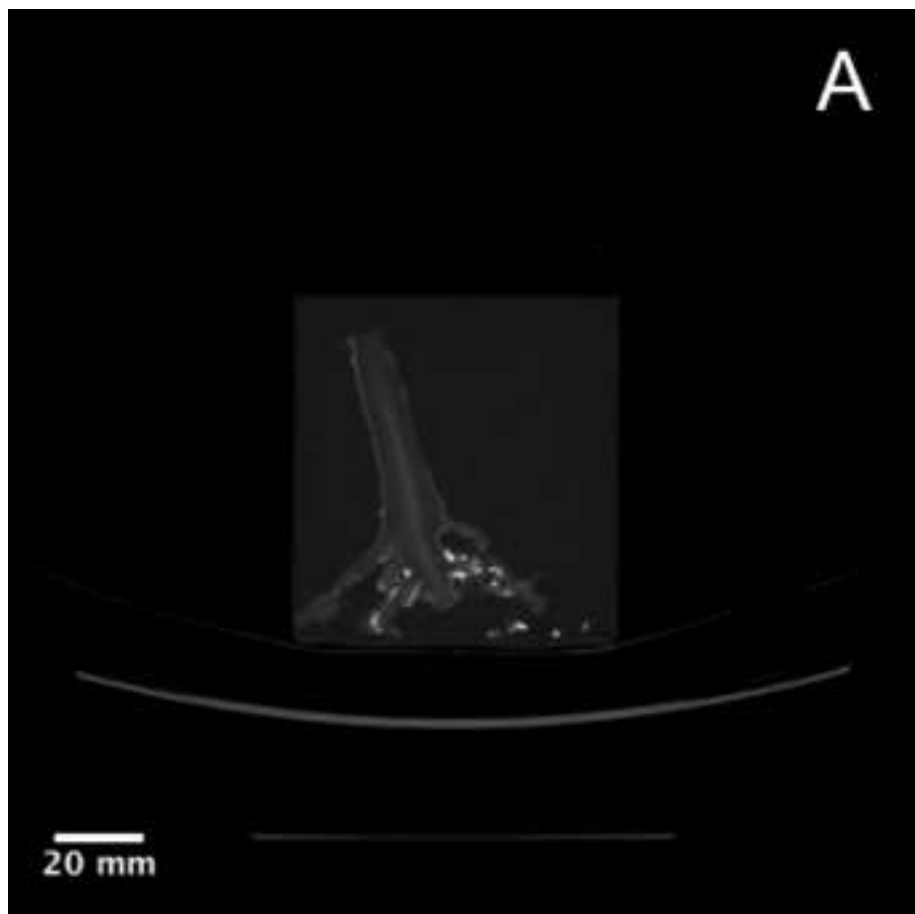


Figure 3
[Click here to download high resolution image](#)

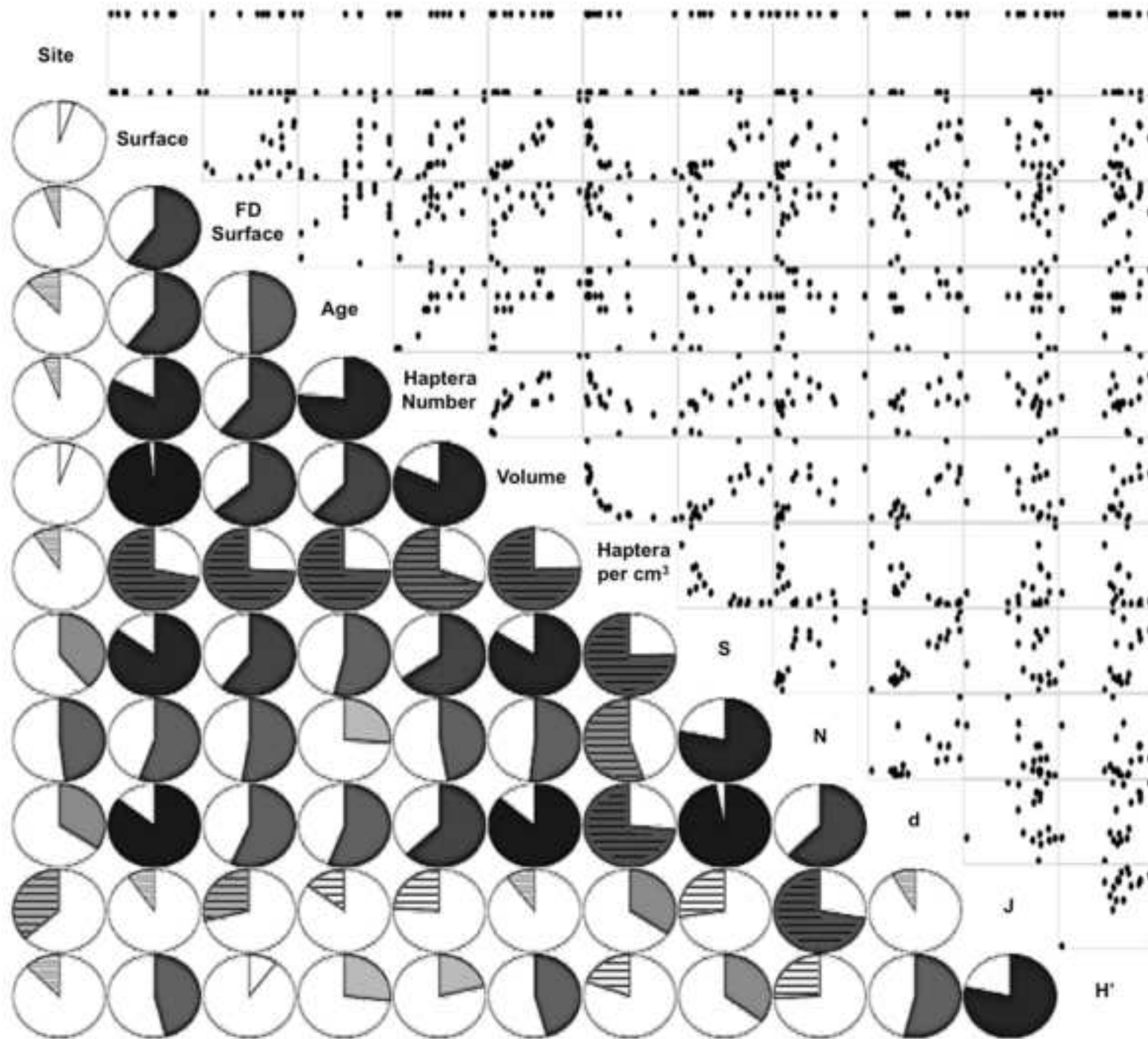


Figure 4
[Click here to download high resolution image](#)

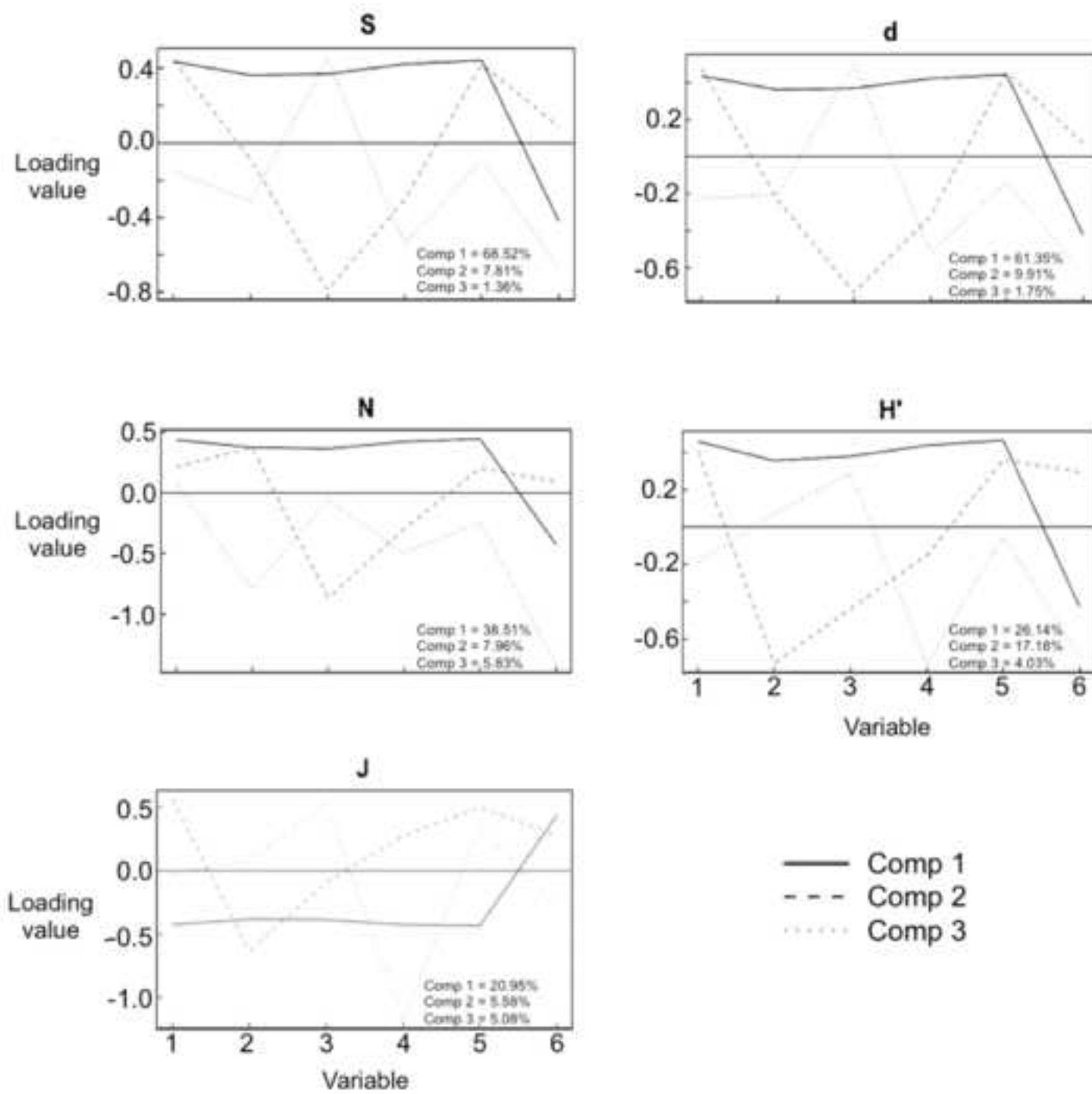


Figure 5
[Click here to download high resolution image](#)

